Perovskites Hot Paper

Deutsche Ausgabe: DOI: 10.1002/ange.201605013
Internationale Ausgabe: DOI: 10.1002/anie.201605013

Low-Energy Electron-Induced Transformations in Organolead Halide Perovskite

Aleksandar R. Milosavljević, Weixin Huang, Subha Sadhu, and Sylwia Ptasinska*

Abstract: *Methylammonium lead iodide perovskite ($MAPbI_3$), a prototype material for potentially high-efficient and low-cost organic–inorganic hybrid perovskite solar cells, has been investigated intensively in recent years. A study of low-energy electron-induced transformations in $MAPbI_3$ is presented, performed by combining controlled electron-impact irradiation with X-ray photoelectron spectroscopy and scanning electron microscopy. Changes were observed in both the elemental composition and the morphology of irradiated $MAPbI_3$ thin films as a function of the electron fluence for incident energies from 4.5 to 60 eV. The results show that low-energy electrons can affect structural and chemical properties of $MAPbI_3$. It is proposed that the transformations are triggered by the interactions with the organic part of the material (methylammonium), resulting in the $MAPbI_3$ decomposition and aggregation of the hydrocarbon layer.*

Organic–inorganic perovskite solar cells have received an immense amount of attention in recent years as one of the most promising photovoltaic materials for solar energy harvesting.[1–6] Their high potential for commercially affordable exploitation is based on a high photon-to-electron conversion efficiency, which has now reached over 20%,[6] and simple, low-cost solution-processed fabrication.[1,7] Exceptional efficiency of organic–inorganic halide perovskites stems from several key attributes, such as high carrier mobility, long diffusion length, and a wide spectral absorption range,[6,8] making them also highly promising materials for different optoelectronic and photovoltaic applications.[6] However, one of the key issues for the application of organic-based perovskite absorbers is their stability during prolonged operation under different conditions.[9] To date, a number of studies have been investigated the transformation/degradation of lead halide perovskites due to the influence of photon irradiation, different environments and the temperature.[9–17] Nevertheless, reports on particle interaction with this material are scarce.

The crystal structure of methylammonium lead iodide perovskite, $CH_3NH_3PbI_3$ ($MAPbI_3$), consists of an inorganic part $(PbI_3)^-$ and an organic part $(CH_3NH_3)^+$. The Pb and I atoms are arranged in an octahedral configuration PbI_6, whereas the positive methylammonium ions $CH_3NH_3^+$ (MA^+) fill the intermediate free spaces between the octahedra, providing charge equilibrium.[6] This organic part of the material might be very susceptible to low-energy electron-induced ionization/fragmentation, which could then lead to distortion of the perovskite crystal structure. As has been demonstrated that interactions of such electrons with molecules in dense media can initiate a variety of chemical reactions, leading to degradation and/or functionalization of surfaces.[18] Therefore, the investigation of low-energy electron interactions with $MAPbI_3$ is important for better understanding of both the structural properties and the radiation damage of the organic–inorganic perovskite solar cells.

Recently, Xiao et al.[19] and Klein-Kedem et al.[20] have investigated high-energy electron-induced damage in perovskite thin films by using cathodoluminescence spectroscopy[19] and scanning electron microscopy (SEM).[20] Xiao et al.[19] found that 2–10 keV electrons can significantly affect perovskite properties and proposed two degradation mechanisms: defect formation caused by electron impact, and phase transformation induced by electron-beam heating.[19] Similarly, Klein-Kedem et al.[20] reported that 1.5–3 keV electrons induced morphological changes in perovskites, exhibiting an exponential degradation as a function of the electron fluence. However, the later studies concern only high-energy electron-induced transformations in $MAPbI_3$. Possible effects due to secondary low-energy electrons, which must be produced, have not been discussed.

Herein, we report a study of low-energy (4.5–60 eV) electron-induced transformations in $MAPbI_3$ thin films, by controllable in vacuo electron irradiation of $MAPbI_3$ samples using an energy-tunable focusing electron gun, followed by ex situ characterization of the irradiated samples using X-ray photoelectron spectroscopy (XPS), scanning electron microscopy (SEM), and X-ray diffraction (XRD). We show that even low-energy electrons (ca. 10 eV) can substantially affect the $MAPbI_3$ crystal structure. We quantify transformations in $MAPbI_3$ as a function of the electron fluence, based on the decrease in nitrogen and iodine contents relative to lead as

[*] Prof. Dr. A. R. Milosavljević, W. Huang, Dr. S. Sadhu, Prof. Dr. S. Ptasinska
Radiation Laboratory
University of Notre Dame, Notre Dame, IN 46556 (USA)
W. Huang
Department of Chemistry and Biochemistry
University of Notre Dame, Notre Dame, IN 46556 (USA)
Prof. Dr. S. Ptasinska
Department of Physics
University of Notre Dame, Notre Dame, IN 46556 (USA)
Prof. Dr. A. R. Milosavljević
SOLEIL, l'Orme des Merisiers
St. Aubin, BP48, 91192 Gif sur Yvette Cedex (France)
E-mail: milosavljevic@synchrotron-soleil.fr
Prof. Dr. A. R. Milosavljević
Institute of Physics Belgrade, University of Belgrade
Pregrevica 118, 11080 Belgrade (Serbia)
Supporting information and the ORCID identification number(s) for the author(s) of this article can be found under http://dx.doi.org/10.1002/anie.201605013.

measured by XPS. Also, by using SEM, we observe significant changes in the morphology of the irradiated $MAPbI_3$ material.

We investigated the elemental decomposition of the irradiated films by measuring the content of N and I relative to Pb, since these elements are hardly present in the ambient environment and thus cannot be adsorbed onto the sample surface (See Sections 1 and 2 of the Supporting Information for more details about the experiment). Figure 1 presents a decrease in the iodine/lead and nitrogen/lead ratios of the irradiated $MAPbI_3$ samples, relative to the control samples, as a function of the electron fluence (F). These results are summarized from a number of different measurements performed over several months. Therefore, the uncertainties of the relative contents may be due to slightly different $MAPbI_3$ preparation parameters, different ex vacuo periods of deposition under possibly different environmental conditions, possible inhomogeneity of thin films, and positions of the XPS sampling spots relative to the irradiated zone. Still, the presented results demonstrate that an electron impact for even as low as 10 eV energy, leads to a substantial transformation of the $MAPbI_3$ material above a fluence of about 10^{16} $e^- cm^{-2}$. Increasing the electron fluence causes the degradation to become severe, leading to a reduction of iodine content from I/Pb ≈ 3 to I/Pb ≈ 2 ($I/I_{control} \approx 0.67$), and a near total loss of N from N/Pb ≈ 1 to N/Pb ≈ 0. The electron-induced degradation was observed even at energies below 10 eV and becomes non-measurable at the energy of about 4.5 eV, for fluences probed up to 3×10^{17} $e^- cm^{-2}$. The reduction of iodine and nitrogen content strongly increases with an increase in the electron energy (Figure 2).

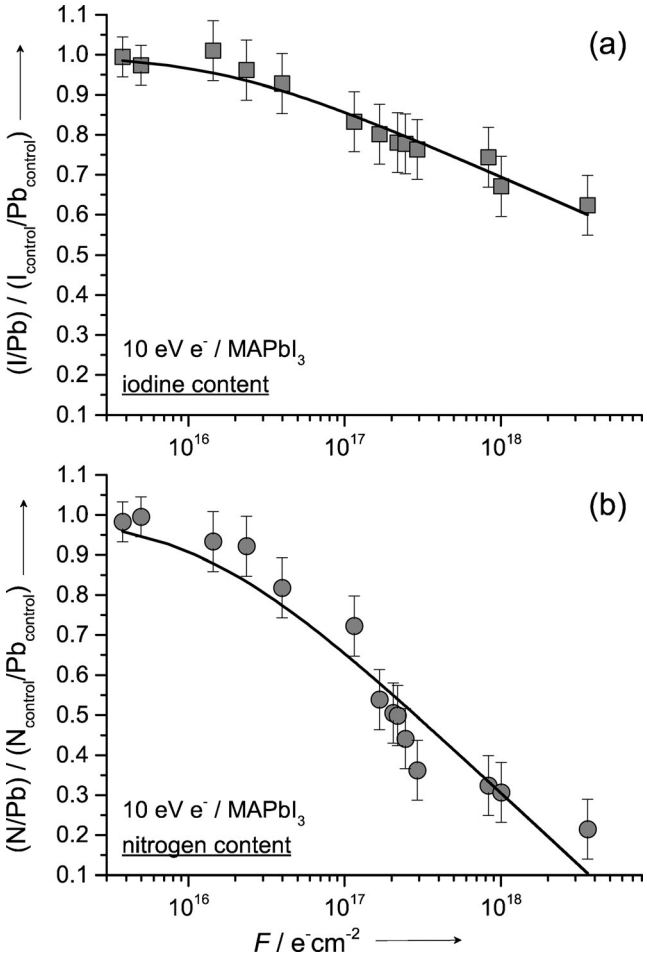

Figure 1. Change of a) iodine and b) nitrogen content relative to lead in the irradiated thin $MAPbI_3$ films, relative to the control samples, as measured using XPS, as a function of 10 eV electron fluence. The control samples underwent the same preparation procedure and were also kept under high vacuum conditions (10^{-6} to 10^{-7} Torr). The absolute errors were obtained according to a mean variation of the measured relative content for a number of different control samples. Full lines represent fitting curves using formula (1), with: a) $C = 0.17 \pm 0.02$; $D = (1.7 \pm 0.7) \times 10^{16}$, b) $C = 0.36 \pm 0.05$; $D = (1.3 \pm 0.6) \times 10^{16}$.

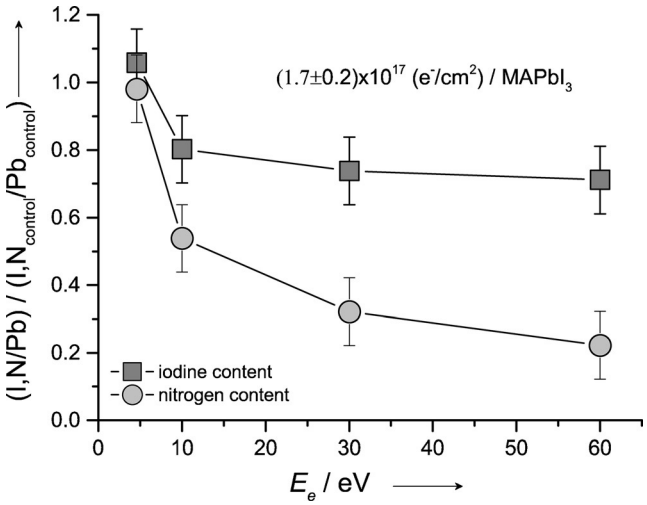

Figure 2. Change of iodine and nitrogen content relative to lead in the irradiated thin $MAPbI_3$ films, relative to the control samples, as a function of the electron energy, at the electron fluence of about $(1.7 \pm 0.2) \times 10^{17}$ $e^- cm^{-2}$, except for the first point at 4.5 eV, which was obtained at the fluence of about 3.2×10^{17} $e^{-1} cm^{-2}$.

The radiation damage of solar cells has been to date investigated for high-energy particles, typically in MeV energy region.[21] Generally, according to extensive experimental research, radiation-induced degradation of solar cell properties follows a logarithmic dependence and can be expressed by the following empirical formula:[21–23]

$$y = 1 - C \log (1 + x/D) \quad (1)$$

where x is the radiation dose or the particle fluence, y is usually the short circuit current or voltage, and C and D are the fitting parameters. We have, therefore, used the same formula (1) to fit the content of I and N in $MAPbI_3$ relative to the control sample (y) as a function of the electron fluence (x). The measured decrease in I and N follows the law given in (1), as shown in Figure 1. Interestingly, the fitting parameter C appears close to that obtained for short-circuit current dependence on the ionizing dose upon high-energy electron-induced damage of amorphous silicon alloy solar cells ($C = 0.6$).[23] Therefore, even the doses at which the properties

of these materials start to markedly change (expressed by D) are different, their relative degradation rates (expressed by C) are comparable.

Figure 3 compares the structure of a pristine sample (a) with those of the control (b) and the irradiated samples (c,d), as examined using SEM (see also the Supporting Information, Figure S4 for lower magnification). The morphology of the control sample already clearly differs from the pristine

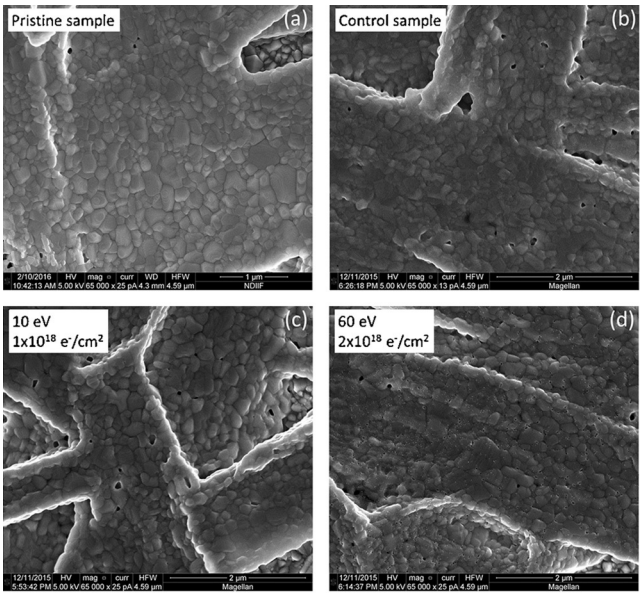

Figure 3. SEM images of a a) pristine sample, b) control sample, c) sample irradiated at 10 eV and fluence of 1×10^{18} $e^{-}cm^{-2}$, and d) sample irradiated at 60 eV and fluence of 2×10^{18} $e^{-}cm^{-2}$.

sample, showing a greater number of pores (Figure 3b). For the incident electron energy of 10 eV and a fluence of about 1×10^{18} $e^{-}cm^{-2}$, some additional morphological changes were seen, such as larger number and size of pores in the $MAPbI_3$ material (Figure 3c) and the sample also becomes more coarsened compared to the control sample. For this sample, a relative decrease in iodine and nitrogen contents was measured using XPS to be about $I_{irradiated}/I_{pristine}=0.7$ and $N_{irradiated}/N_{pristine}=0.3$, respectively. However, the electron irradiation at the incident energy of 60 eV and a fluence of about 2×10^{18} $e^{-}cm^{-2}$ induced severe macroscopic changes in the $MAPbI_3$ layer (Figure 3d). Indeed, a large number of pores and cracks were formed over the whole scanned area, leading to a total transformation of the morphology of the $MAPbI_3$ film. The surface of the film became rougher owing to the presence of a number of pinhole-like pores. For this sample, the measured relative decrease in iodine and nitrogen was about $I_{irradiated}/I_{pristine}=0.68$ and $N_{irradiated}/N_{pristine}=0.05$, respectively. The SEM images clearly show that low-energy electron irradiation may induce significant changes in the morphology of the $MAPbI_3$ material. It should be noted, however, that only the surface of $MAPbI_3$ samples was affected by the present low-energy electron irradiation experiments, as confirmed by X-ray diffraction (XRD) analysis (see Section 4 of the Supporting Information).

The experimental results show that high electron fluences result in the loss of one nitrogen and one iodine atom from $MAPbI_3$: $N/Pb=1\rightarrow N/Pb=0$ and $I/Pb=3\rightarrow I/Pb=2$. Certainly, the transformation is caused by electron impact and cannot be due to interactions with other molecules (for example, water), since samples are kept under high-vacuum conditions (10^{-6}–10^{-7} Torr). We can also exclude both mechanisms proposed for keV electron beam damage of $MAPbI_3$ (direct defect formation and phase transformation induced by electron-beam heating).[19] Indeed, the local radiation power density is about eight to nine orders of magnitude lower in the present case (ca. 10^{2}–10^{3} $W m^{-2}$) than in the experiment of Xiao et al.[19] (ca. 10^{11} $W m^{-2}$). Also, at low incident energies, the ionization effect should dominate over displacements.[19,22,23] It should be noted that the radiation-induced degradation decreases with a decrease in the incident energy and becomes hardly measurable at about 4.5 eV, which is close to the calculated HOMO binding energy of MA^{+} in defect-free bulk perovskites (4.5–5 eV).[8]

Therefore, we propose that low-energy electron-induced degradation of $MAPbI_3$ is triggered by electron impact dissociative ionization of methylammonium ion MA^{+} ($CH_3NH_3^{+}$), which results in breakage of the C–N bond. The average bond dissociation enthalpy for the dissociation of MA along the C–N bond: $CH_3NH_3\rightarrow CH_3+NH_3$ was recently calculated at 3.17 eV,[8] therefore this reaction is energetically possible in the present experiment and should represent the most favorable MA^{+} dissociation channel.[8] Moreover, such electron-induced dissociation of MA directly leads to the formation of stable volatile ammonium NH_3 product, which can explain the decrease in N content in the sample ($N/Pb\rightarrow 0$). Interestingly, Delugas et al.[8] proposed that MA in $MAPbI_3$ could dissociate into ammonia and iodomethane (NH_3+CH_3I), which remain attached and preserve the perovskite structure. However, this possibility is excluded in the present study, since we clearly measured the loss of both N and I from the sample. The present results thus indicate that electron interactions with the $MAPbI_3$ thin film lead to the formation of PbI_2 and a polymer hydrocarbon complex that aggregates on the surface, while gaseous species NH_3 and HI escape from the sample and are evacuated:

$$CH_3NH_3PbI_3 \xrightarrow{e^{-}\rightarrow C-N\ \text{breakage}} (-CH_2-) + NH_3\uparrow + HI\uparrow + PbI_2 \qquad (2)$$

The present interpretation (2) is in accord with the one recently proposed by Li et al.[24] to explain decomposition of $MAPbI_3$ upon water exposure. Note that low-energy electron-induced synthesis in condensed mixed organic layers has been frequently observed and characterized previously.[18]

The detailed XPS analysis of the carbon content was performed to confirm reaction (2). The XPS signal in carbon 1s region of a pristine $MAPbI_3$ sample typically yields a broad photoelectron feature, which is composed of two peaks (Supporting Information, Figure S6), which correspond to 1s ionization of C–N carbon (286.6 eV) from the $CH_3NH_3^{+}$ ion of the $MAPbI_3$ sample and C–H carbon (285.3 eV) from hydrocarbons inevitably present on the sample surface as contamination.[25,26] In our measurements, these two peaks are of similar intensities for the pristine samples (Supporting

Information, Figure S6 a–d), as well as control samples (for example, Figure 4 a). However, electron irradiation drastically changes this ratio, resulting in a strong decrease in the perovskite C–N carbon peak relative to C–H (Figures 4 b–d), thus confirming chemical transformation of the irradiated surface area due to intensive C–N bond cleavage. Moreover, this reduction of the C–N peak intensity directly depends on both the electron fluence and the incident energy, in accordance with the decrease in I and N content (Figure 2).

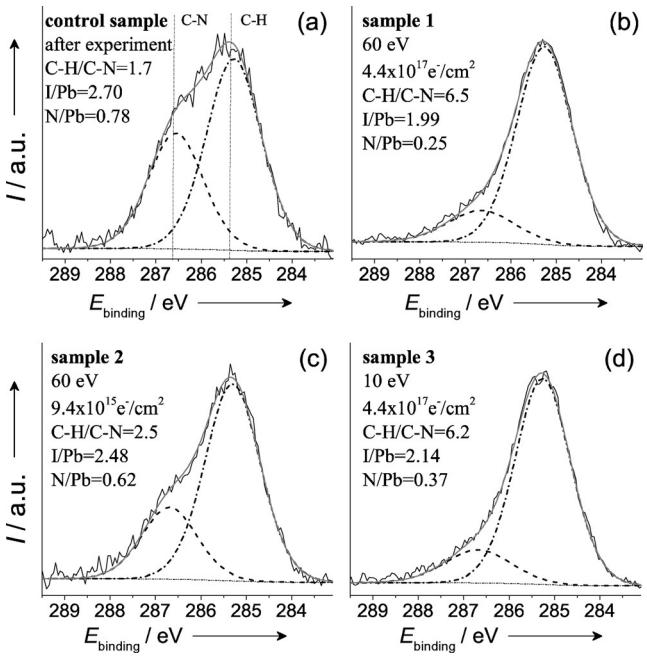

Figure 4. C 1s XPS of the a) control and b)–d) three irradiated $CH_3NH_3PbI_3$ samples.

Apart from a drastic signal decrease in C–N relative to those for the C–H bonding, the total carbon content (C–N + C–H) relative to lead actually strongly increases upon electron irradiation. For example, for Sample 1 in Figure 4 b and the Supporting Information, Figure S6 (b,f), the atomic ratio (C–N + C–H)/Pb increased about 2.5 times upon irradiation. A tentative explanation is that the electrons affect the surface of the sample and, since XPS also probes only a 5–10 nm thick surface layer, the polymerization (2) leads to an apparent increase in the C–H signal. This conclusion was scrutinized by analyzing a perovskite sample submitted to extremely high electron fluence (ca. 1×10^{20} $e^- cm^{-2}$) and at high electron energy of 60 eV (see Section 6 of the Supporting Information). A dark spot was formed on the perovskite surface that corresponds to direct electron beam irradiation. The XPS performed on this spot could detect only a strong carbon peak corresponding to C–H bonding, whereas the content of all other elements, including Pb, was zero. Since Pb cannot disappear from the sample, the most logical explanation is that the intensive electron irradiation produces a hydrocarbon layer that prevents XPS analysis due to limited escape depth of photoelectrons.

In conclusion, we have shown that low-energy electrons induce significant transformations in methylammonium lead iodide perovskite. The degradation of the material strongly increases with an increase in both the radiation dose (fluence) and the electron energy from 4.5 eV (no detectable degradation even above 10^{17} $e^- cm^{-2}$) to 60 eV (severe degradation already above 10^{17} $e^- cm^{-2}$). We propose that the observed degradation of $MAPbI_3$ starts with electron-induced C–N bond breakage in MA^+, which eventually leads to the escape of gaseous species (NH_3 and HI) and formation of PbI_2 and polymer hydrocarbon residue ($-CH_2-$) on the surface. The present results are important to better understand the properties of organic lead halide perovskites, as potential solar cell absorbers, particularly the role of low-energy electron induced processes (excitation and ionization of the organic component). Moreover, the present study shows that secondary low-energy electrons may strongly contribute to the radiation damage in organic–inorganic perovskites.

Acknowledgements

All authors would like to acknowledge the Division of Basic Energy Sciences, Office of Science, US Department of Energy grant number DE-FC02-04ER15533. This is contribution number NDRL 5113 from the Notre Dame Radiation Laboratory. A.R.M. acknowledges support by MESTD RS (Project No. 171020). We thank Milos Rankovic for help with SIMION simulations.

Keywords: low-energy electrons · organolead compounds · perovskite · solar cells · X-ray photoelectron spectroscopy

How to cite: *Angew. Chem. Int. Ed.* **2016**, *55*, 10083–10087
Angew. Chem. **2016**, *128*, 10237–10241

[1] H. J. Snaith, *J. Phys. Chem. Lett.* **2013**, *4*, 3623–3630.
[2] J. S. Manser, P. V. Kamat, *Nat. Photonics* **2014**, *8*, 737–743.
[3] H. Zhou, Q. Chen, G. Li, S. Luo, T.-B. Song, H.-S. Duan, Z. Hong, Y. Liu, Y. Yang, *Science* **2013**, *27*, 238–242.
[4] N. J. Jeon, J. H. Noh, Y. C. Kim, W. S. Yang, S. Ryu, S. Seok, *Nat. Mater.* **2014**, *13*, 1–7.
[5] N. J. Jeon, J. H. Noh, W. S. Yang, Y. C. Kim, S. Ryu, J. Seo, S. Seok, *Nature* **2015**, *517*, 476–480.
[6] Q. Chen, N. De Marco, Y. Yang, T.-B. Song, C.-C. Chen, H. Zhao, Z. Hong, H. Zhou, Y. Yang, *Nano Today* **2015**, *10*, 355–396.
[7] J. A. Sichert, Y. Tong, N. Mutz, M. Vollmer, S. Fischer, K. Z. Milowska, et al., *Nano Lett.* **2015**, *15*, 6521–6527.
[8] P. Delugas, A. Filippetti, A. Mattoni, *Phys. Rev. B* **2015**, *92*, 045301.
[9] G. Niu, X. Guo, L. Wang, *J. Mater. Chem. A* **2015**, *3*, 8970–8980.
[10] J. F. Galisteo-López, M. Anaya, M. E. Calvo, H. Míguez, *J. Phys. Chem. Lett.* **2015**, *6*, 2200–2205.
[11] G. Niu, W. Li, F. Meng, L. Wang, H. Dong, Y. Qiu, *J. Mater. Chem. A* **2014**, *2*, 705–710.
[12] B. Philippe, B.-W. Park, R. Lindblad, J. Oscarsson, S. Ahmadi, E. M. J. Johansson, H. Rensmo, *Chem. Mater.* **2015**, *27*, 1720–1731.
[13] A. Alberti, I. Deretzis, G. Pellegrino, C. Bongiorno, E. Smecca, G. Mannino, F. Giannazzo, G. G. Condorelli, N. Sakai, T. Miyasaka, et al., *ChemPhysChem* **2015**, *16*, 3064–3071.

[14] W. Huang, J. S. Manser, P. V. Kamat, S. Ptasinska, *Chem. Mater.* **2016**, *28*, 303 – 311.
[15] J. A. Christians, P. A. Miranda Herrera, P. V. Kamat, *J. Am. Chem. Soc.* **2015**, *137*, 1530 – 1538.
[16] A. Dualeh, N. Tétreault, T. Moehl, P. Gao, M. K. Nazeeruddin, M. Grätzel, *Adv. Funct. Mater.* **2014**, *24*, 3250 – 3258.
[17] G. Divitini, S. Cacovich, F. Matteocci, L. Cinà, A. Di Carlo, C. Ducati, *Nat. Energy* **2016**, 15012.
[18] E. Böhler, J. Warneke, P. Swiderek, *Chem. Soc. Rev.* **2013**, *42*, 9219 – 9231.
[19] C. Xiao, Z. Li, H. Guthrey, J. Moseley, Y. Yang, S. Wozny, H. Moutinho, B. To, J. J. Berry, B. P. Gorman, et al., *J. Phys. Chem. C* **2015**, *119*, 26904 – 26911.
[20] N. Klein-Kedem, D. Cahen, G. Hodes, *Acc. Chem. Res.* **2016**, *49*, 347 – 354.
[21] S. R. Messenger, G. P. Summers, E. A. Burke, R. J. Walters, M. A. Xapsos, *Prog. Photovoltaics* **2001**, *9*, 103 – 121.
[22] *GaAs Solar Cell Radiation Handbook* (Ed.: B. E. Anspaugh), JPL, Pasadena, **1996**, pp. 5.1 – 5.7.
[23] S. Sato, K. Beernink, T. Ohshima, *Jpn. J. Appl. Phys.* **2015**, *54*, 061401.
[24] Y. Li, X. Xu, C. Wang, C. Wang, F. Xie, J. Yang, Y. Gao, *J. Phys. Chem. C* **2015**, *119*, 23996 – 24002.
[25] S. Chen, T. W. Goh, D. Sabba, J. Chua, N. Mathews, C. H. A. Huan, T. C. Sum, *APL Mater.* **2014**, *2*, 081512.
[26] L. Liu, J. A. McLeod, R. Wang, P. Shen, S. Duhm, *Appl. Phys. Lett.* **2015**, *107*, 061904.

Received: May 22, 2016
Published online: June 29, 2016

